Nitrogen-doped carbon-coated hollow SnS_2/NiS microflowers for high-performance lithium storage

Junhai Wang[1], Jiandong Zheng (✉)[1], Liping Gao[1], Qingshan Dai[2], Sang Woo Joo (✉)[3], and Jiarui Huang (✉)[2]

1 School of Material and Chemical Engineering, Chuzhou University, Chuzhou 239000, China
2 Key Laboratory of Functional Molecular Solids of the Ministry of Education, College of Chemistry and Materials Science, Anhui Normal University, Wuhu 241002, China
3 School of Mechanical Engineering, Yeungnam University, Gyeongsan, Gyeongbuk 38541, Republic of Korea

E-mails: jrhuang@mail.ahnu.edu.cn (J.H.), zjd071@126.com (J.Z.), swjoo@yu.ac.kr (S.W.J.)

Supplementary material

1 Material characterizations

The crystal structures of samples were determined by X-ray diffraction (XRD; Shimadzu XRD-6000) using high-intensity Cu Kα radiation (1.54178 Å), and the morphologies and element distributions by scanning electron microscopy (SEM; Hitachi S8100), and energy-dispersive X-ray spectroscopy (EDS). Transmission electron microscopy (TEM; Hitachi HT-7700) and high-resolution transmission electron microscopy (HRTEM; JEOL-2010 TEM) were used to determine the sample microstructures. The Raman spectra were obtained using a Renishaw inVia Raman spectrometer and a 532 nm laser source. The Brunauer–Emmett–Teller (BET; Micromeritics ASAP 2460) specific surface and pore volumes of samples were measured. Thermogravimetric analysis (TGA; Setaram Labsys Evo SDT Q600) was performed at a heating rate of 10 °C·min^{-1} from room temperature to 400 °C in flowing air. X-ray photoelectron spectroscopy (XPS; ESCALAB 250) was used to analyze the surface elemental compositions and chemical bonding.

2 Assembly and testing of lithium-ion batteries

Lithium metal (0.6 mm in thickness, 15.8 mm in diameter, and 99.95% purity) was used as the opposite electrode of the button-type CR2032 half battery, and polypropylene film (Celgard 2400) was used as the diaphragm. The prepared active electrode was composed of 80 wt.% active material (SnS_2/NiS and SnS_2/NiS@N–C), 10 wt.% conductive carbon black (analytically pure), and 10 wt.% sodium carboxymethyl cellulose (CMC; analytically pure). The weighed active substance and conductive carbon black were ground with a mortar and pestle. A certain quality of the binder CMC was added, and a few drops of styrene butadiene rubber (SBR) were added with stirring until a sticky consistency was reached. The slurry was coated with copper foil and dried under vacuum at 80 °C for 24 h. The electrode sheet was cut into a circle sheet with 12 mm in diameter. The mass loadings of the active mass among SnS_2/NiS@N–C and SnS_2/NiS anodes were approximately 1.92

and 1.88 mg·cm^{-2}, respectively. Finally, the battery assembly work was performed in an argon-filled glove box (Miller, Ltd., $c(O_2)$ < 0.01 ppm, $c(H_2O)$ < 0.01 ppm). The solvent in the electrolyte was diethyl carbonate/dimethyl carbonate/vinyl carbonate (the corresponding volume ratio was V(DEC):V(DMC):V(EC) = 1:1:1) with 1 mol·L^{-1} $LiPF_6$ of lithium salt. On the battery rack equipped with the Neware BTS 2300 system (Shenzhen, China), the voltage was set within 0.01–3.0 V. The battery voltammetry (I–U) and electrochemical impedance (EIS) tests were performed using an electrochemical workstation (ChenHua CHI-660E, frequency from 100 kHz to 10 Hz).

Table S1 Cycling properties comparison of SnS_2/NiS@N–C and recently reported electrodes

Electrode material	Capacity/(mAh·g^{-1})	Current density/(A·g^{-1})	Cycle number	Ref.
SnS_2/C_3N_4	444.7	0.1	100	[52]
SnS_2/CNTs	551	0.1	100	[53]
NiS/CNT	515	0.1	30	[54]
NiS/graphene	446	0.2	50	[55]
NiSn@C	445	0.2	400	[56]
Sn–Ni–Cu–alloy@carbon nanorods	490	0.45	400	[57]
Ni–Sn-based hybrid composite	510	1.0	100	[58]
SnS–ZnS@C	992	0.2	100	[59]
Hollow SnS_2/NiS@N–C microflowers	667.9	0.2	200	this work
	403.5	2.0	200	

Table S2 Simulation model with the estimated values

Electrode material	R_1/Ω	R_2/Ω	R_{ct}/Ω
SnS_2/NiS@N–C (initial)	2.3	–	53.8
SnS_2/NiS@N–C (after 200 cycles)	3.1	18.3	113.5
SnS_2/NiS (initial)	4.1	–	96.0
SnS_2/NiS (after 200 cycles)	3.7	24.2	147.7

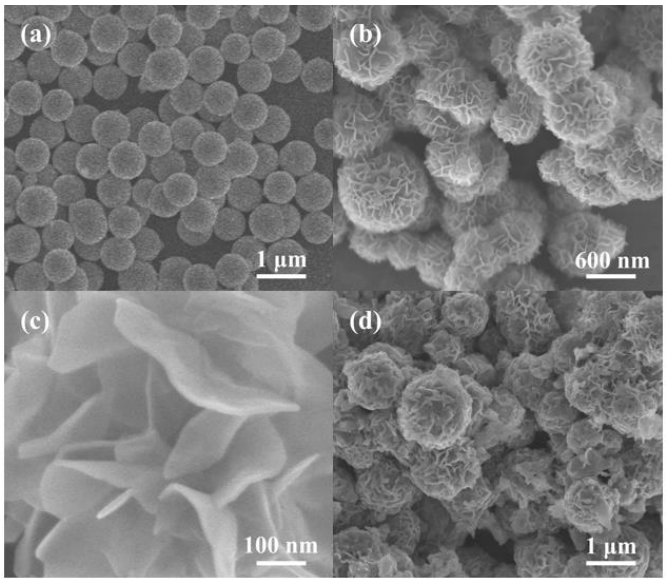

Fig. S1 SEM images of **(a)** $NiSn(OH)_6$ spheres, **(b)(c)** hollow SnS_2/NiS microflowers, and **(d)** hollow SnS_2/NiS@N–C microflowers.

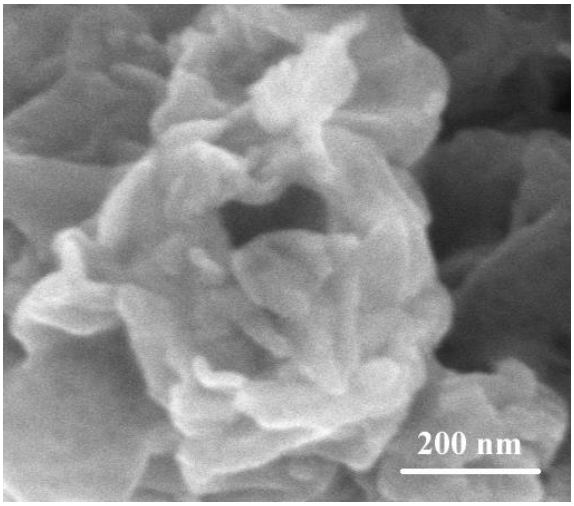

Fig. S2 High-magnification SEM image of hollow SnS_2/NiS@N–C microflowers.

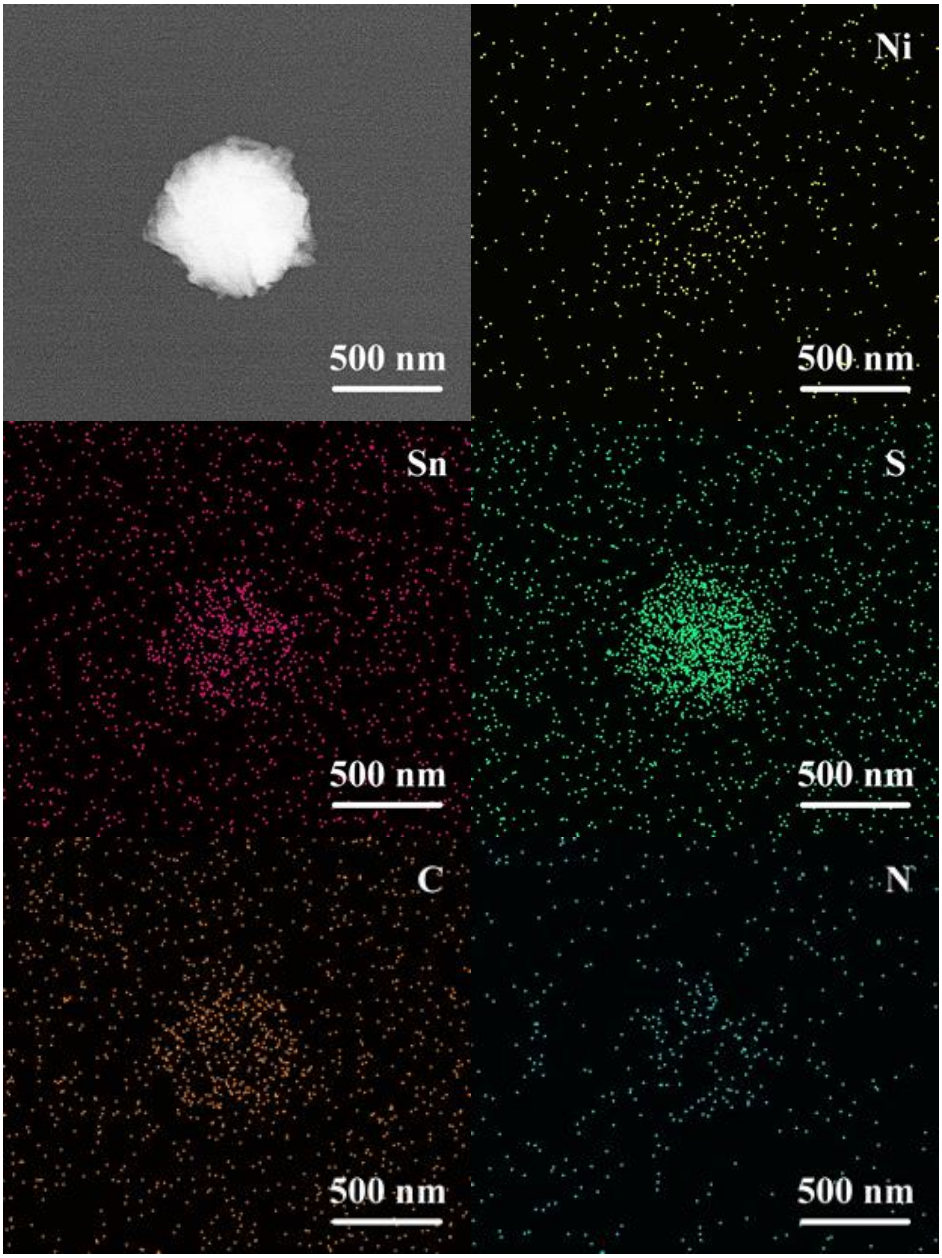

Fig. S3 Elemental mapping images of hollow SnS_2/NiS@N–C microflowers.

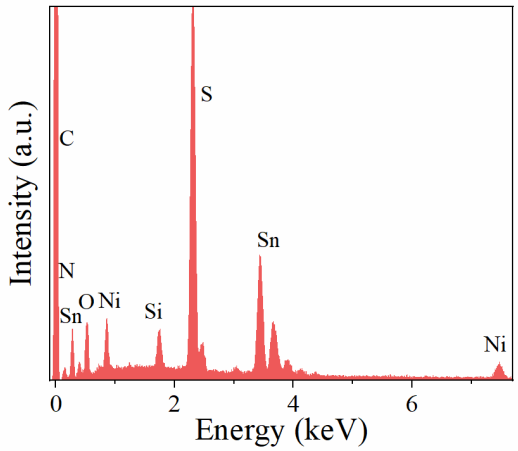

Fig. S4 EDS analysis of hollow SnS_2/NiS@N–C microflowers.

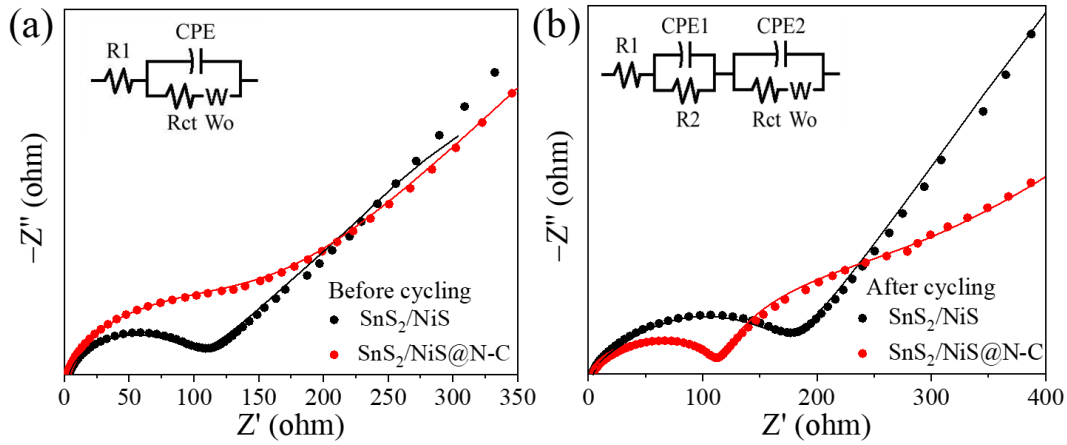

Fig. S5 Nyquist plots of hollow SnS_2/NiS@N–C and SnS_2/NiS microflower anodes **(a)** before the cycling test and **(b)** after 200 cycles (insets are corresponding simulation circuit models).

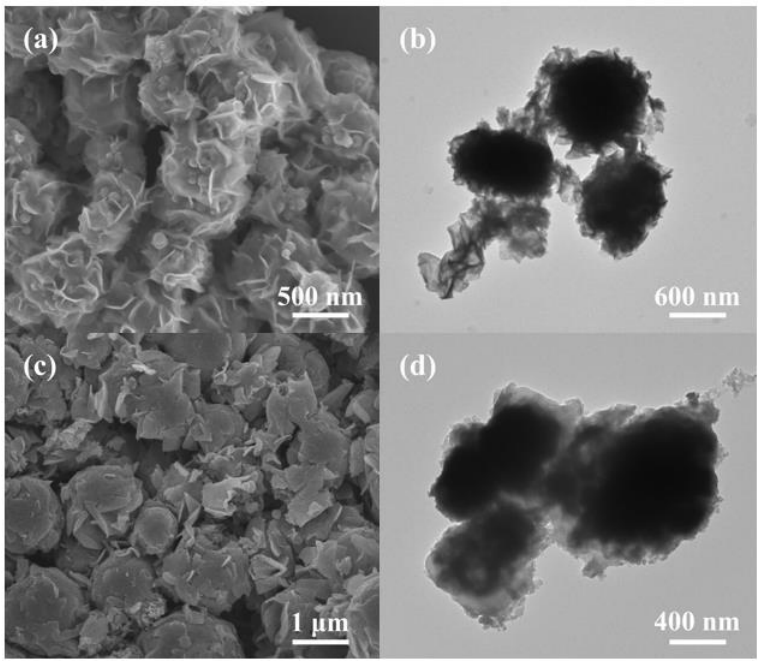

Fig. S6 (a) SEM and **(b)** TEM images of SnS_2/NiS@N–C anode after cycling test. **(c)** SEM and **(d)** TEM images of SnS_2/NiS anode after cycling test.

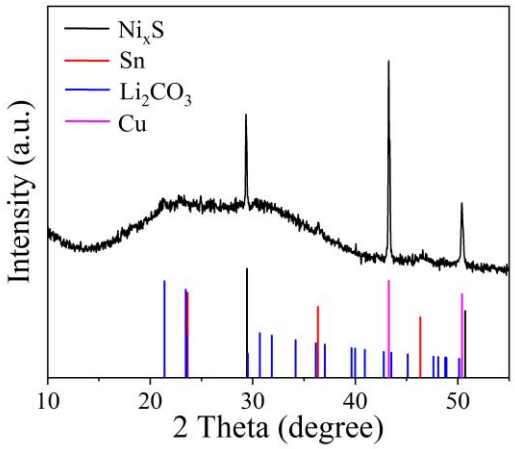

Fig. S7 XRD pattern of SnS_2/NiS@N–C anode after cycling test.

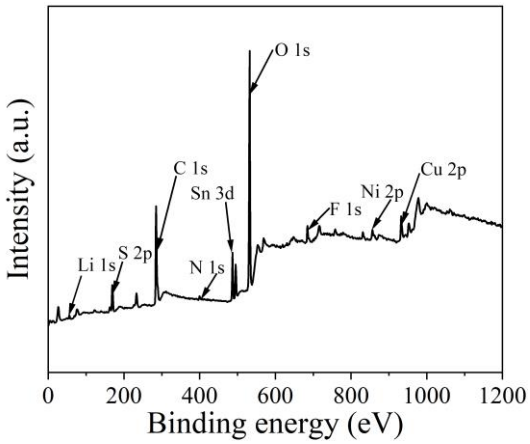

Fig. S8 XPS survey spectrum of the SnS_2/NiS@N–C anode after cycling test.